Anal Bioanal Chem (2002) 374 : 619–625
DOI 10.1007/s00216-002-1505-6

SPECIAL ISSUE PAPER

R. Fischer

Depth profiles and resolution limits in accelerator-based solid state analysis

Received: 26 February 2002 / Accepted: 24 July 2002 / Published online: 18 September 2002

Abstract A ubiquitous problem in solid state analysis is the determination of the elemental composition of a sample as a function of the depth. The determination of the depth profiles from ion-beam experiments is an ill-posed inversion problem due to ion-beam and detector-induced energy spreads as well as energy-loss straggling and small-angle scattering effects. The inversion problem is solved in the framework of Bayesian probability theory, which provides a method for quantifying and combining uncertain data and uncertain additional information. By deconvolving the apparatus transfer function and modeling the scattering events in the sample we reconstructed depth profiles of ^{13}C in tetrahedral amorphous carbon (ta-C) and depth profiles in $^{12}C/^{13}C$ marker probes. An enhancement of the energy resolution by a factor of 6 was obtained.

Keywords Depth profiles reconstruction · Resolution enhancement · BPT

Introduction

Ion-beam diagnostics are routinely used for quantitative analysis of the surface composition of mixture materials up to a depth of a few μm. Rutherford backscattering spectroscopy (RBS) and elastic recoil detection (ERD) are commonly applied to determine the depth-dependent elemental composition of the sample. However, the interpretation of the spectra may be hampered by overlapping structures due to resolution limitations and due to the ambiguity of elements in different depths. The limited energy resolution due to ion-beam and detector-induced energy spreads as well as energy-loss straggling and small-angle scattering effects restrict the mass and depth resolution. To determine the depth profile we have to determine the apparatus function including all energy broadening effects. Thin multi-layer mixture systems are capable of measuring the apparatus function as a function of the depth.

The paper is intended to give an estimate of the practical limitations of resolution enhancement and to summarize applications of resolution enhancement and depth profile reconstructions from other papers of the author. We summarize the method of Bayesian probability theory (BPT) to deconvolve the apparatus function and to reconstruct distributions from ill-posed inversion problems. Additionally, we show the practical limits of resolution enhancement. We also illustrate the method in three applications: resolution enhancement, reconstruction of depth profiles of ^{13}C in tetrahedral amorphous carbon (ta-C), and depth profiles in $^{12}C/^{13}C$ marker probes.

R. Fischer (✉)
Centre for Interdisciplinary Plasma Science,
Max-Planck-Institut für Plasmaphysik, EURATOM Association,
85748 Garching bei München, Germany
e-mail: rainer.fischer@ipp.mpg.de

Theory

Ill-posed inverse problems

Distribution reconstruction is an inverse problem in which the data $\boldsymbol{d}=d_1,...,d_M$ are related to the distribution $f(x)$ via the functional $\mathcal{A}$ and distorted by noise ε, $d_i=\mathcal{A}(\{f(x)\},y_i)+\varepsilon_i$, where the datum d_i is taken at coordinate y_i. For the two applications of resolution enhancement and depth profiles of ^{13}C in ta-C, $\mathcal{A}$ describes the convolution of $f(x)$ with an apparatus function A,

$$d_i = \sum_{j=1}^{N} A_{ij} f_j + \varepsilon_i, \tag{1}$$

where for practical reasons $f(x)$ is discretized, $f_j, j=1,...,N$. In general, $\mathcal{A}$ can be any function of $f(x)$, as is the case in our application of reconstructing the depth profiles of a $^{12}C/^{13}C$ marker probe. The inverse problem of determining $\boldsymbol{f}$ from the data $\boldsymbol{d}$ is ill-posed when $\boldsymbol{f}$ is not uniquely determined by the data. The direct inversion of Eq. (1) leads to meaningless results, since the statistical error ε is amplified by the small eigenvalues of A, which is illustrated for the first application of resolution enhancement. Noisy data allow for ambiguity in $\boldsymbol{f}$ within the uncertainty

level of the data. To overcome this problem and to separate the signal from the noise, the statistical nature of the error has to be taken into account and the distribution of interest has to be regularized with additional information.

Bayesian probability theory

BPT provides a general and consistent mathematical tool for logical inference. BPT is fundamental to all scientific work, as it provides in Bayes theorem, that is, a formal rule for updating knowledge in the light of new data and conditioning information I

$$P\,(\mathbf{f}|\,\mathbf{d},\,I) = \frac{P\,(\mathbf{d}|\,\mathbf{f},\;I)\,P\,(\mathbf{f}|\,I)}{P\,(\mathbf{d}|\,I)}. \tag{2}$$

Bayes theorem relates the *posterior* probability density function (pdf) $P(\boldsymbol{f}|\boldsymbol{d},I)$ to the *likelihood* pdf $P(\boldsymbol{d}|\boldsymbol{f},I)$ and the *prior* pdf $P(\boldsymbol{f}|I)$. The notation with the vertical bar denotes conditional probabilities, or 'given', and the comma is read as the conjunction 'and'. Bayes theorem allows one to combine noisy (uncertain) measured data $\boldsymbol{d}$ with additional information I independent of the data. Since both the data and the additional information may be uncertain, we have to assign probabilities to quantify the plausibility of each being true. The historical terms "posterior" and "prior" have a logical, rather than a temporal, meaning. They simply mean "with" and "without" the new data taken into account. A recommendable tutorial on BPT is given by Sivia [1].

In order to apply Bayes' theorem we need a likelihood pdf and a prior pdf. The likelihood function is the probability for getting the observed data supposing that the correct distribution is $\boldsymbol{f}$. It describes the uncertainties associated with the experimental data. In the case of a counting experiment with a large number of counts, we are dealing with a Gaussian likelihood function with variance $\sigma^2_i \approx d_i$,

$$p\,(\mathbf{d}\,|\mathbf{D}\,,\sigma) = \prod_{i=1}^{M} \frac{1}{\sqrt{2\pi}\,\sigma_i} \exp\left(-\frac{(d_i - \mathcal{A}\,(\{f\,(x)\}\,,\,y_i))^2}{2\sigma_i^2}\right) \tag{3}$$

A modification of the variance $\sigma^2{}_i$ allows one to combine the uncertainty of the apparatus function, A_{ij}, with the uncertainty of the data where the uncertainties of A_{ij} are denoted δ_{ij} [2]:

$$\sigma_i^2 \Rightarrow \sigma_{\mathrm{eff},i}^2 = \sigma_i^2 + \sum_{j=1}^{N} \delta_{ij}^2 f_j^2 \tag{4}$$

The least-informative prior pdf for distributions is the entropic prior which allows one to quantify the information content of a distribution [3, 4]. We want to reconstruct depth profiles that reflect the significant information content in the data, and we do not want to fit the noise in the data. The entropic prior penalizes depth profiles according to their information content. Recently, we showed that the entropic prior is not sufficient to avoid noise fitting completely since the entropy does not allow for correlations in the reconstruction [5]. Since each distribution consists of regions with different length scales, we incorporated the concept of local smoothness as additional prior information in the Bayesian framework. Details about the adaptive maximum entropy concept can be found elsewhere [6].

Resolution limits

An often posed question is: Are there theoretical or practical limitations of resolution enhancement by numerically deconvolving the apparatus function from the data? The achievable resolution enhancement depends on the uncertainty of the data and the uncertainty of the apparatus function to be deconvolved. The uncertainty (error) of the data can often be reduced by more or longer measurements. The number of measurements being realized is usually limited by time and money but can also be restricted by basic physical mechanism. Our ERD application for high-resolution depth profiling of ^{13}C at an ultrathin film of ta-C shows that the occurrence of irradiation damage restricts the ion fluency and hence the statistic of the data. The uncertainty of the apparatus function may also be due to statistical uncertainties of the measurement. In addition, unrecovered effects or unspecified details in the apparatus function may contribute to its uncertainty, often called *systematic errors*. Most commonly, the apparatus function is assumed to be described by a function with parameters incorporated into the fitting routine such as a Gaussian with the variance as additional parameter. This approach is not recommended because tiny differences between the true and the modeled apparatus function may cause mock structures in the deconvolved result that may be interpreted erroneously. Preferably, the apparatus function is measured on samples reflecting the broadening mechanism directly, as done for the present applications. The uncertainties of the measured apparatus function can be combined with the uncertainties of the data to be deconvolved, as shown in Eq. (4).

To assess the limits of resolution enhancement we assume a distribution f and an apparatus function A, both normalized, centered at the origin, and variance $var(f)$ and $var(A)$, respectively. Applying the convolution theorem results in

$$\mathrm{var}(d) = \mathrm{var}(A) + \mathrm{var}(f) \tag{5}$$

To get an idea of the experimental effort necessary to obtain a resolution enhancement by a factor ξ let $width(f) = width(d)/\xi$ where $width^2 \propto var$:

$$\left(1 - \frac{1}{\xi^2}\right) \mathrm{var}(d) = \mathrm{var}(A) \tag{6}$$

A resolution enhancement factor $\xi=6$ gives $width(d)=(1+0.014)width(A)$. The measurement must allow one to distinguish a difference of 1.4% in the widths of the apparatus function A and the measured data d. An enhancement factor of $\xi=10$ ($\xi=50$) can only be obtained when the difference between the widths of A and d can be distinguished on a level of 0.5% (0.02%), respectively. Various applications analyzed by the author have shown that a res-

olution enhancement factor of ξ=6–8 is achievable with well-known apparatus functions. A larger factor requires very refined experiments in both the data and the apparatus function.

Applications

Resolution enhancement

To illustrate an ill-posed problem and to show typical resolution enhancements in ion-beam experiments Fig. 1a shows RBS spectra of thin Cu and Co films evaporated on Si substrates. Both films have a thickness of a few atomic layers to obtain sufficient intensity as well as negligible multiple scattering. Details of the experiment can be found elsewhere [7]. The Co spectrum reflects the apparatus function A since Co is isotopically pure, that is, it consists of only one atomic mass. The uncertainty of the apparatus matrix A, δ_{ij}, is given by the statistical uncertainty of the Co data. The goal is to deconvolve the Cu data with the apparatus function measured with the Co data.

The deconvolved distribution in Fig. 1b is obtained by maximizing the likelihood function without constraints (constant prior pdf). The result show huge oscillations which are due to noise fitting. Even with positivity constraints, $\boldsymbol{f}>0$, the result (Fig. 1c) is disappointing because the peaks show pointwise oscillations. Figure 1d depicts the result of the adaptive maximum entropy method allowing for adaptive smoothing. The two isotopes ^{63}Cu and ^{65}Cu are clearly resolved. The FWHM of the dominant ^{63}Cu peak after deconvolution is about six times smaller than the experimental resolution and beyond any conceivable experimental resolution with semiconductor detectors. The smaller peak of ^{65}Cu is slightly broader because the signal-to-noise ratio is lower. The measured abundances of the isotopes are 70.1% ^{63}Cu and 29.9% ^{65}Cu. This has to be compared with the natural abundance of 69.2% ^{63}Cu and 30.8% ^{65}Cu.

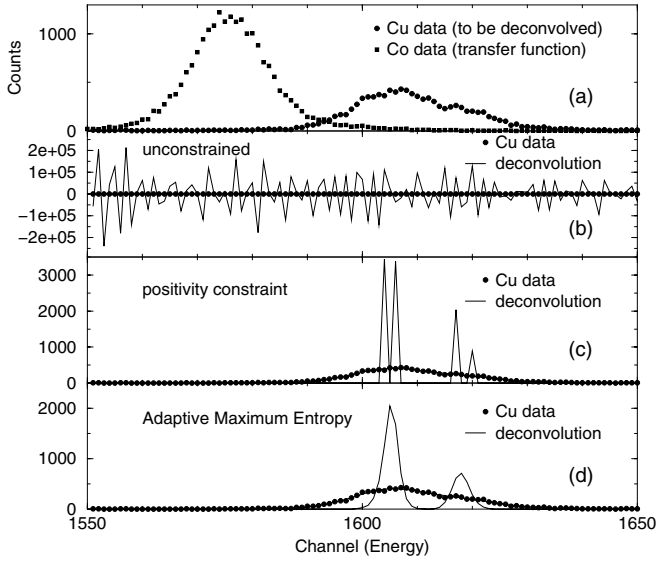

Fig. 1a–d RBS spectra of a thin Cu film (*dots*) and of a thin Co film (*squares*) evaporated on Si substrates (**a**), the deconvolved distribution obtained by maximizing the likelihood function without constraints (**b**), with positivity constraints (**c**), and the deconvolution result obtained with the adaptive maximum entropy method (**d**)

Depth profile of ^{13}C in ta-C

Elastic recoil detection analysis (ERDA) was applied for high-resolution depth profiling of ^{13}C at an ultra-thin film of tetrahedral amorphous carbon (ta-C). High-resolution ERDA allows one to resolve single monolayers if heavy ion beams with energies of about 0.5 A MeV (e.g., 60 MeV ^{127}I) are utilized ([8] and references therein). With the Munich Q3D magnetic spectrograph in combination with a new focal-plane detector it was possible to reduce the irradiation damage to a level at which ultra-thin layers or small fractions of an atomic layer can be measured with negligible alterations of the profiles. Another problem with using ERDA for depth profiling is that depth resolution decreases with increasing depth due to energy-loss straggling and small-angle scattering effects. To improve the depth resolution the measured spectra have to be deconvolved with respect to an apparatus function which contains all effects of ion-beam and detector-induced energy spreads as well as energy-loss straggling and small-angle scattering effects.

In recent years, ta-C materials are of great interest due to extreme properties such as high hardness, high resistivity, optical transparency, chemical inertness, and good thermal stability. The material is sp^3 hybridized in the short distance and amorphous in the long range. Thin-film growth of ta-C is only possible with techniques involving energetic ions in a small energy range of 50 eV to 1 keV. Below and above this energy range the amount of sp^2-bonded carbon atoms increases and the diamond-like phases diminish. The ion-energy dependence on the formation of diamond-like phases has been subjected to experimental and theoretical studies, but the nucleation and growth mechanisms of ta-C and the strong ion-energy dependence have not been well understood [9].

To provide experimental data for improving existing models of thin-film growth of dense, diamond-like materials we have analyzed mean ion ranges and mixing zones involved in ion-beam deposition of ta-C using high-resolution ERDA. Three different types of ta-C films were deposited onto Si(100) substrates as sketched in Fig. 2. The left panel shows a film where about 12 nm ^{12}C were deposited with ion energy E_{ion} (e.g., 40 eV and 230 eV) and, subsequently, 5×10^{14} at cm^{-2} ^{13}C (about 0.06 nm) were deposited with the same E_{ion}. These types of samples allow one to obtain information about the dependence of the implantation depth on E_{ion}. The middle panel shows a film where an additional film of 7 nm ^{12}C (about 1×10^{17} at cm^{-2} ^{12}C) was deposited with E_{ion}. These samples allow one to investigate mixing zones obtained during ta-C growth by measuring the spreading of the ^{13}C interfacial

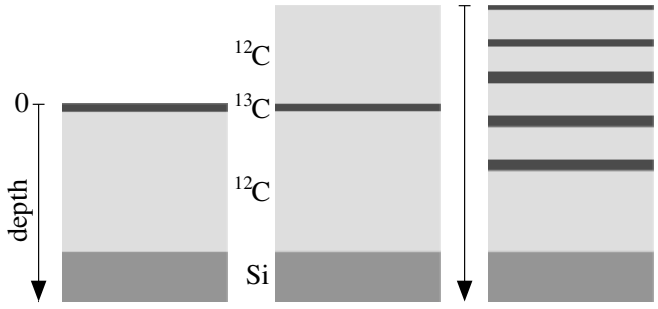

Fig. 2 A sketch of the three different types of ta-C films: a thin ^{13}C layer on ^{12}C for the determination of implantation depths (*left panel*), an additional ^{12}C layer for measuring the mixing behavior (*middle*), and a multi-layer for the determination of the depth-dependent apparatus function (*right*)

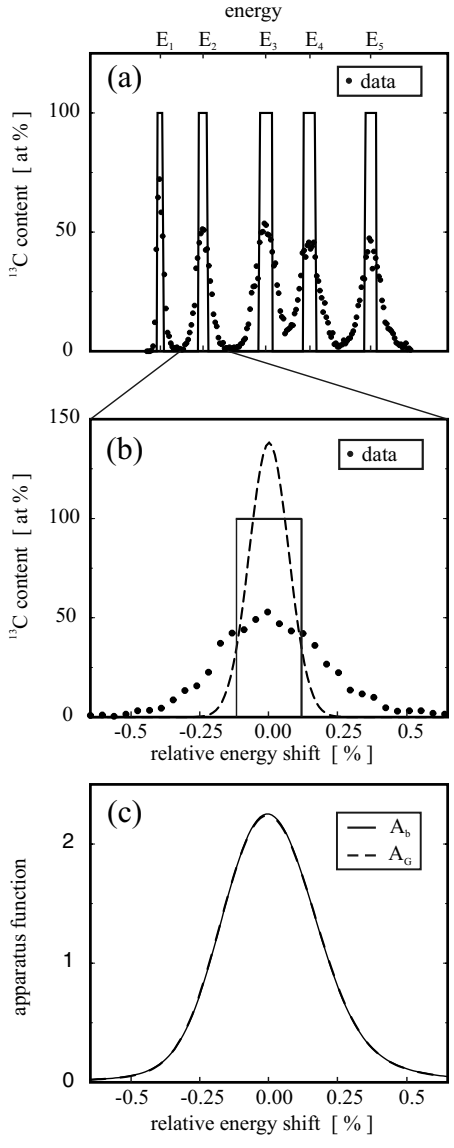

Fig. 3a–c ERD spectrum of the multi-layer film and a box-shaped intrinsic depth profile (**a**), a Gaussian with the same variance as the box (**b**), and the deconvolved apparatus functions (**c**) for the depth of the second layer assuming the box-shaped intrinsic depth profile (*solid line*) and the Gaussian (*dashed*)

layer. The right panel shows a thermally grown (electron beam evaporation) multi-layer consisting of ^{12}C layers about 1 μg cm^{-2} thick and ^{13}C layers about 0.1 μg cm^{-2} thick. Assuming a box-shaped intrinsic depth profile (Fig. 3a), the depth-dependent apparatus function was deconvolved from the measured ERD spectrum of ^{13}C (Fig. 3c). The estimation of the apparatus function is robust because deconvolving a box-shaped profile or a Gaussian with the same variance (Fig. 3b) results in very similar apparatus functions (Fig. 3c). Details of the estimation of the apparatus function can be found elsewhere [8].

The implantation ranges of the low-energy carbon ions are shown in Fig. 4 for E_{ion}=40 eV and 230 eV. The solid line depicts the deconvolution of the data (dots) with the depth-dependent apparatus function determined with the multi-layer experiment. The dashed line shows the deconvolution with an apparatus function calculated with the DEPTH code ([8]) which systematically under-estimates the width of the apparatus function. The ^{13}C profiles reveal non-symmetric structures where the surface slopes are steeper than the bulk slopes. In addition, the profile implanted with E_{ion}=230 eV shows a shoulder which can be barely recovered from the sparse raw data. The right side of Fig. 4 shows a sketch of the profiles of ^{13}C for the two implantation energies.

Figure 5a shows the ^{13}C mixing profile for E_{ion}=40 eV after an additional implantation of 7 nm ^{12}C (middle panel of Fig. 2). The profile is much wider compared to the deconvolved reconstruction of the corresponding surface profile due to mixing of the ^{13}C layer during ^{12}C sub-plantation. In addition, there is a small amount of ^{13}C at the surface. Figure 5b depicts the profiles corresponding to the maximum (solid line) and the mean (dotted line) of the posterior probability with its confidence interval of ± one standard deviation. The dependence of the implantation depths, widths, and uncertainties on E_{ion} are derived from the widths of the deconvolved profiles and the respective confidence intervals.

ERDA on the Munich Q3D magnetic spectrograph together with the numerical method of deconvolving the depth-dependent apparatus function allows us to resolve elemental depth profiles at the physical limit of single atomic layers. The estimation of the uncertainty of the quantity of interests in the framework of BPT is crucial for comparison with model calculations of the system ta-C.

Depth profile of a $^{12}C/^{13}C$ marker probe

RBS is a frequently used technique for the analysis of erosion measurements of plasma facing materials in ASDEX Upgrade fusion experiments ([10] and references therein). The fusion experiment is concerned with investigating the physical basis of a fusion power plant. Like the sun, such a plant is to generate energy from fusion of atomic nuclei. One of the main goals is to investigate the confinement of high-temperature hydrogen plasmas (about 10^8 K in the plasma center and 10^4–10^5 K at the plasma edge) in

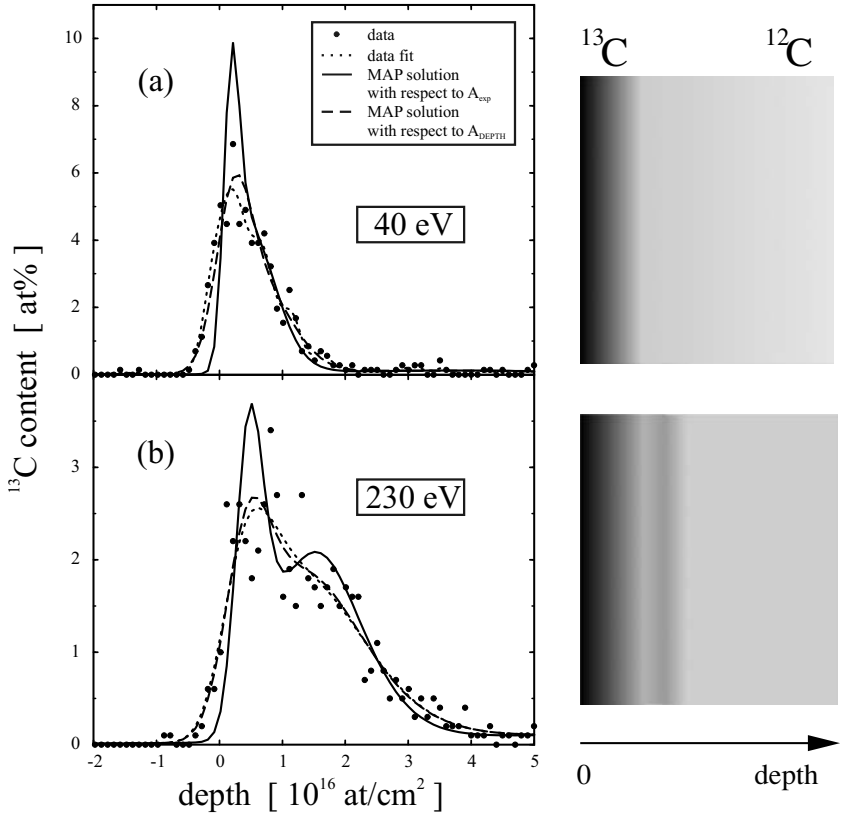

Fig. 4a,b ERD spectra (*dots*) for ^{13}C implanted with E_{ion}=40 eV (**a**) and E_{ion}=230 eV (**b**), deconvolution with the depth-dependent apparatus function determined with the multi-layer experiment (*solid line*) and with an apparatus function calculated with the DEPTH code (*dashed*). The *right side* shows a sketch of the profiles of ^{13}C for the two implantation energies

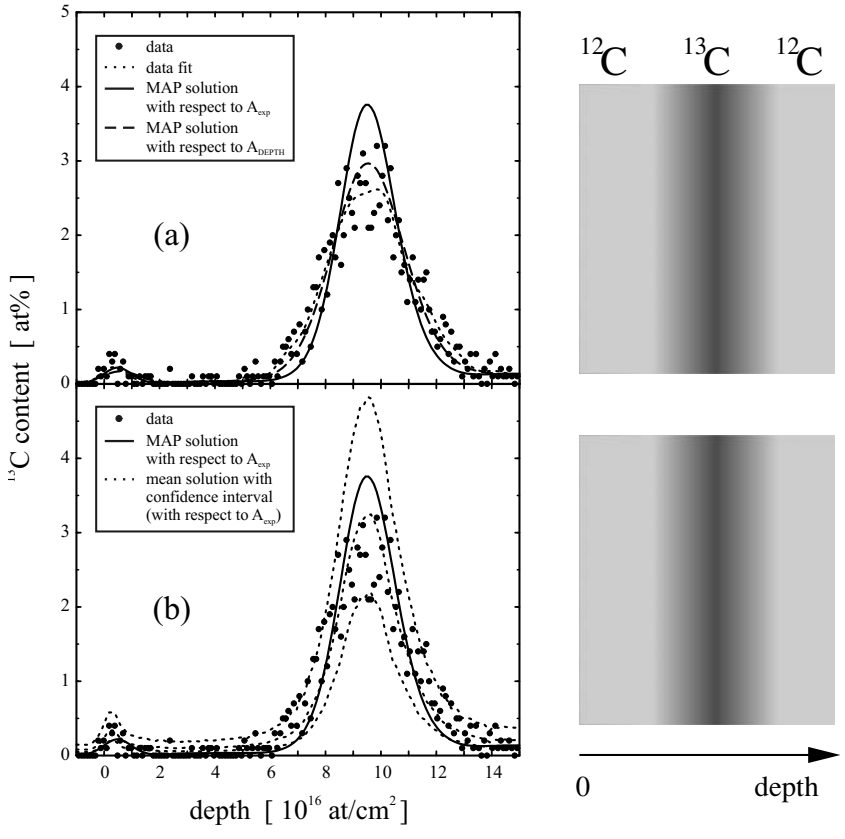

Fig. 5 **a** ERD spectra (*dots*) for ^{13}C after an additional implantation of ^{12}C (E_{ion}=40 eV), deconvolution with the experimental (*solid line*) and calculated (*dashed*) apparatus function, and **b** the maximum (*solid line*) and the mean (*dotted line*) of the posterior probability with its confidence interval of ± one standard deviation

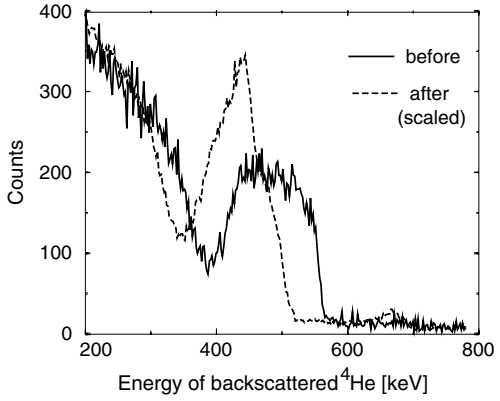

Fig. 6 RBS spectra before and after plasma exposure. The shift of the high-energy edge indicates that at the surface ^{13}C is superposed by ^{12}C

magnetic fields. The hot central plasma is well separated from the surrounding first wall. Energetic particles (1 eV–10 keV) can, however, still leave the confined plasma and interact with the surrounding materials. The material properties of the plasma facing components are modified by ion implantation, erosion, and deposition of material from other wall areas. Modeling material migration and understanding the complex interaction processes between the plasma and the wall materials is important for the integration of optimized plasma facing components in fusion devices.

To determine carbon erosion rates, graphite probes covered with a 150 nm layer of ^{13}C were exposed to a single plasma discharge of about 4 s. ^{13}C was used because chemical erosion is unaffected by isotope substitution. In addition, the electronic stopping power in ^{13}C and ^{12}C is the same which prevents complications due to the limited accuracy of the stopping power. The apparatus function is determined with a RBS spectrum of a thin Co film on a Si substrate. The statistical uncertainty of the apparatus function modifies the variance in Eq. (4). Details of the system can be found elsewhere [10].

Figure 6 shows RBS spectra measured with 2.0 MeV ^{4}He ions before and after plasma exposure. The difference of the RBS spectra before and after exposure contains the information about the erosion and re-deposition yields. Before plasma exposure the signal from the ^{13}C layer at 430–580 eV is separated from the signal from the ^{12}C bulk material beneath the ^{13}C layer. After plasma exposure the high-energy edge of the ^{13}C signal has shifted towards lower energies (500 eV). This indicates that there is no longer ^{13}C at the surface of the sample. The peak at 430 eV is caused by ^{12}C at the sample surface and by ^{13}C below the surface. Depth profiles are no longer uniquely determined which prevents standard analysis software for RBS depth profiling to produce reasonable results.

Figure 7 shows the reconstructed ^{12}C and ^{13}C depth profiles before and after plasma exposure. The depth is expressed in terms of area atom density. The sample was divided in 23 layers with a thickness of 150×10^{15} atoms cm^{-2}. Before plasma exposure the surface concentration

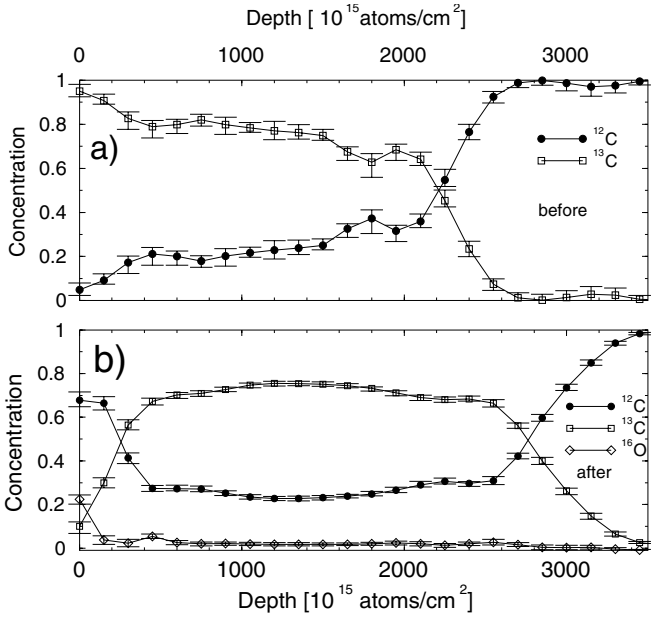

Fig. 7a,b ^{12}C and ^{13}C depth profiles before (**a**) and after (**b**) plasma exposure with asymmetric confidence intervals

of ^{13}C is >70%. The remaining 10–30% consists of ^{12}C caused by impurities in the coating process. After plasma exposure the depth profiles have changed dramatically. A ^{12}C layer with a thickness of about 250×10^{15} atoms cm^{-2} is on top of the ^{13}C layer. The thickness of the ^{13}C layer did not change but the ^{13}C surface enrichment disappeared. The conclusion is that during the plasma exposure ^{12}C was deposited on the sample. Since the thickness of the ^{13}C layer was unaffected there was no erosion. The disappearance of the ^{13}C surface enrichment indicates a mixing zone where the impinging ^{12}C atoms intermix with the ^{13}C layer. This conjecture is supported from the small amount of ^{16}O, which forms, after carbon, the second largest impurity fraction of the ASDEX Upgrade hydrogen plasma.

Summary

A resolution enhancement with numerical methods is limited to a factor of about 10. An enhancement factor of 6–8 can be routinely achieved with well-known apparatus functions. The reconstructions of depth profiles at the physical limit of a few atomic layers were obtained by deconvolving the depth-dependent apparatus broadening functions determined from multi-layer samples. Bayesian probability theory allows one to estimate the most probable depth profiles together with the confidence intervals.

References

1. Sivia DS (1996) Data analysis – A Bayesian turorial. Clarendon Press, Oxford
2. Dose V, Fischer R, von der Linden W (1998) In: Erickson G, Rychert J, Smith R (eds) Maximum entropy and Bayesian methods. Kluwer Academic, Dordrecht, pp 147–152

3. Skilling J (1991) In: Buck B, Macaulay VA (eds) Maximum entropy in action. Clarendon Press, Oxford, p 19
4. Fischer R, von der Linden W, Dose V (1996) In: Silver RN, Hanson KM (eds) Maximum entropy and Bayesian methods. Kluwer Academic Publishers, Dordrecht, p 229
5. Fischer R, von der Linden W, Dose V (1996) In: Sears M, Nedeljkovic V, Pendrock NE, Sibisi S (eds) MAXENT96 – Proceedings of the Maximum Entropy Conference. NMB Printers, Port Elizabeth, South Africa, p 21
6. Fischer R (1999) In: Kluge W (ed) Proceedings of the workshop on physics and computer science. Christian-Albrechts-University, Kiel, Germany
7. Fischer R, Mayer M, von der Linden W, Dose V (1997) Phys Rev E 55:6667
8. Neumaier P, Dollinger G, Bergmaier A, Genchev I, Görgens L, Fischer R, Ronning C, Hofsäss H (2001) Nucl Instrum Methods Phys Res Sect B 183:48
9. Hofsäss H, Feldermann H, Merk R, Sebastian M, Ronning C (1998) Appl Phys Lett 66:513
10. Toussaint UV, Fischer R, Krieger K, Dose V (1999) New J Phys 1:11